ISSN: 2277-3754
ISO 9001:2008 Certified
International Journal of Engineering and Innovative Technology (IJEIT)
Volume 3, Issue 7, January 2014

Mathematical and Geometrical Formulation/Analysis for Beam Divergence Limit Angle in Radiotherapy Wedges

F Casesnoves MSc (Physics) MD
Computational Bioengineering Researcher
SIAM (Society for Industrial and Applied Matematices) & ASME (American Society of Mechanical Engineering) Denver, Colorado State, USA

Abstract: ***Wedge filters constitute a useful type of Beam Modification Devices (BMD) in Radiation Therapy. Its use is routinary in both Forward and Inverse Treatment Planning Optimization (ITPO). In previous contributions we presented the exact/approximated path of a Pencil Photon-Beam (AAA Model, Anisothropic Analytic Algorithm), through standard manufacturing alloy wedges. It was found a so-defined Limit-Angle (LA), beyond of which the outpoint of the beam is located improperly at the lateral side of the wedge. LA exists because of the photon-beam physical divergence phenomenon. In this paper we carry out the Geometrical and Analytical determination of the LA in function of the beam divergence angle, collimator output distance, and the size parameters of the wedge filter. Two methods are used, Geometrical and Analytical. Boundaries formulation is presented with inequalities. A series of Mathematical Formulations for LAs, is shown with basic approximations according to the industrial manufacturing wedge standards. In addition, an extension of these geometrical approximations is applied on so-called Conformal wedges (CW) [11.1, 11.2]. A primary stage for CW Limit Angle is determined. Formulation is verified with Optimization Mathematical Methods.***

Keywords: **AAA, ITPO, BMD, Static Wedge Filters, Nonlinear Optimization, Analytic Geometry, Industrial Manufacturing Standards (IMS), Conformal Wedge (CW).**

I. INTRODUCTION

Wedge filters are commonly used in RT Treatment Planning Optimization (TPO), Forward and Inverse Methods. Its function is to conform the tumor shape, and avoid hot spots without excessive technical effort, usually for superficial cancer (e.g., Larynx, Breast, Lung, or Prostate tumors) [11, 11.1, 11.2]. Wedges belong to the generic group of Beam Modification Devices (BMD) [33], which constitutes a useful type of technical resources in TPO. It is not unusual to combine Multi Leaf Collimator modification with wedge filters (wedges, virtual wedges, universal wedges and other techniques), to carry out an optimal adaptation of the dose delivery within the Tumor Target. Among the recent techniques for wedge filters we find the omniwedge filter [41].

In addition to the principal mechanical and physical tools and parts of the new accelerators, the complementary use of Beam Modification Devices (BMDs) are useful to get conformal dosage and avoid hot spots without excessive technical effort. The inconvenient of the BMDs is the dose distribution alteration, due mainly to the increment of scattering photons (more frequent in Kilo voltage than Megavoltage). BMD types are classified [Sharma, 2011] by Shielding, Compensation, Wedge Filtration and Flattering. There are a number of BMDs, among them; those most frequently used are Multileaf Collimators (MLC), Shielding, Compensators, Wedge Filters, and Penumbra Trimmers. We focus this paper on Wedge Filters, which are used in general for relatively superficial tumors. Wedges can be classified as: Universal, Dynamic, Virtual, and Pseudo-Wedges [33].

The use of wedges is justified for practical, technical and economic reasons. High-quality alloy materials are not expensive, and the size of the wedges makes their handling, change and substitution easy. Manufacturing of wedge filter series with different angles (usually **15°,30°,45°,60°**) is neither difficult nor expensive. Alloy is a high-endurance material which provides long industrial life for continuous RT sessions. In addition, several combinations of wedges in 2D and 3D configurations, the so-called omniwedge system, may be used to obtain a series of radiation distribution(s) to adapt the dose delivery to the tumor shape with accurate approximations and engineering precision.

Attenuation dose of the wedge (exponential factor, Eq [22]), depends mainly on the beam path through the wedge material, the material composition itself, and proportionality on the beam divergence angle [11]. Previously, [11], an exact/approximated geometrical calculation of this path was published for the AAA Model in 3D/2D, so-called Anysothropic Analytical Algorithm [3439], with acceptable RMS error values in general. These formulas depend on the beam divergence angle (BDA), among other parameters. Basic simulations were also shown to determine error attenuation factors within the integral dose formula of the AAA algorithm.

However, apart from the path length and geometrical approximations, we consider the path through the wedge as dependent also on the BDA [6-11]. This fact implies that BDAs could become a technical problem if the beam approaches the lateral borders, when passing throughout the filter. In such cases, it could happen that the outpoint of the

ISSN: 2277-3754
ISO 9001:2008 Certified
International Journal of Engineering and Innovative Technology (IJEIT)
Volume 3, Issue 7, January 2014

beam is improperly located at the lateral side of the wedge. Symmetrical distribution of the incident beam over the wedge surface, without approaching too much the wedge borders, is desirable for precision/accuracy in the Treatment Plan. It was found in simulation data, a so-defined Limit Angle (LA), beyond of which this inconvenient physical-geometrical phenomenon could occur [11.1,11.2]

Photon-Beam divergence angles values vary around 20 degrees. The Beam minimum divergence depends on the collimator design quality, and in general of the precision engineering manufacturing of the LINACs.

In this technical paper we present a series of geometrical and analytical formulas for LA determination in standard wedge filters. Mathematical developments were tried to be shown clear, complete, and understandable. In addition, coordinate systems could be used/modified for other Radio-therapy Dosimetry Models, apart from the classical AAA algorithm [35, 36].

II. LIMIT ANGLE FOR GENERAL DIVERGENCE ANGLE

This Section deals with the methods used to define mathematically the LA from a geometrical and analytical point of analysis.

1.-Algebraic Geometry Approximations and Geodesics

In Fig 1 we draw the line that joints P (LINAC collimator output) with the inferior wedge border and intersects the axis u_2 at $u_1 = 0$. The distance r at u_2 axis by similar triangles is given by similar triangles, since the equation of the inferior plane [11] is

$$z = tg\alpha(u_1 + a);$$

[Ref 11]

therefore

$$\frac{(P+z)}{b} = \frac{P}{r};$$

[Equation 1]

then,

$$r = \frac{(b \cdot P)}{(P+z)} = \frac{(b \cdot P)}{(P + \tan\alpha \cdot a)};$$

[Eq 2]

Now we rotate the equation of the line P-r along the superior wedge surface 90 degrees to reach the axis u_1 (Fig 2) when $u_2=0$. If so, there is an inferior geodesic at the surface of the cylinder of b radius (Fig 3). This inferior geodesic is defined by the intersection of cylinder and wedge inferior plane (Fig 3). The lowest value of θ corresponds to the values [11.1],

$$u_2 = 0; u_1 = r]_{u_2=0}$$

[Eq 3]

Since the radius of cylinder is b, at that point we have,

$$z = \tan\alpha(b + a);$$

[Eq 4]

Therefore, this minimum angle is the LA, because if we take any other higher value along the inferior geodesic, the angle would be higher, and the beam output could go beyond the inferior geodesic. This angle is useful for any value of u_1 and u_2 . So we get

$$r\Big]_{u_2=0} = b \cdot P\left[\frac{1}{(\tan\alpha \cdot (b+a) + P)}\right]$$

[Eq 5]

then,

$$\tan(\theta_L) = \frac{(r]_{u_2=0})}{P};$$

[Eq 6]

and the resulting formula is

$$\theta_L\left[Geometrical\right] = arctg\,\frac{(r]_{u_2=0})}{P};$$

[Eq 7]

According to Figs 1,2,3, in general, the radius of the superior wedge surface geodesic is by trigonometry,

$$\frac{b}{r} = \frac{(\tan\alpha \cdot (u_1 + a) + P)}{P};$$

or

$$r = b \cdot P \cdot \left[\frac{1}{(P + \tan\alpha \cdot (u_1 + a))}\right];$$

[Eqs 8]

The subsequent step is to define the equations of the geodesic that set the limit angle over the superior surface of the wedge. We will define a geodesic which guarantees the previous defined θ_L [Geometrical] holds, and a general curve described by the conditions of Figs 1 and 2. Taking the length of the distance at u_2 defined in Fig 2, we get

$$\frac{P}{r} = \frac{(P + \tan\alpha \cdot (u_1 + a))}{b};$$

then

$$r = b \cdot P \cdot \left[\frac{1}{(P + \tan\alpha \cdot (u_1 + a))}\right];$$

[Eqs 9]

ISSN: 2277-3754
ISO 9001:2008 Certified
International Journal of Engineering and Innovative Technology (IJEIT)
Volume 3, Issue 7, January 2014

This circle over the superior surface makes sure that the pencilbeam is correctly conducted. But it is also useful to define r in function of θ, such as

$$\tan\theta = \frac{r}{P};$$

[Eq 10]

then from the previous expression

$$r = b - \tan\theta \cdot [\tan\alpha \cdot [b + a]] = r(\theta);$$

[Eq 11]

If we follow the same method with the data of Figs 1 and 2, the curve described by the beam whose output is at inferior geodesic of Fig 3 is given by the equation

$$r = b - \tan\theta \cdot \left[\tan\alpha \cdot \left[\sqrt{(b^2 - u_2{}^2)} + a\right]\right] = r(\theta);$$

[Eq 12]

and we have used the constraint for inferior geodesic

$$u_1{}^2 + u_2{}^2 = b^2;$$

[Eq 13]

2.-Analytical Minimization. IMRT Voxel-Beamlet Discretization/Approximation.

The analytical proof that θ_L [geometrical] is a minimum is based on the fact that when L (Figs, 1,2,3), is maximum, θ_L is minimum. The output of the beam path is always at or into the geodesic of the cylinder of radius b. Then, at any point of the cylinder geodesic

$$u_1{}^2 + u_2{}^2 = b^2;$$

[Eq 14]

and

$$L^2 = f(u_2) = b^2 + \left(P + \tan\alpha \cdot \left(\sqrt{(b^2 - u_2{}^2)} + a\right)\right)^2;$$

[Eq 15]

If we maximize this function, we find a maximum for u_1 =b, with the second derivative for this value positive. It is necessary to consider in this maximization that P is in the negative direction of axis Z. Then, the result of maximum for u_1 =b holds. Therefore, we have proven that this LA [geometrical] is minimum and applicable to all directions to avoid output of beam at lateral sides of the wedge. That is, the maximization is,

$$\frac{\partial f(u_2)}{\partial u_2} = 0$$

and

$$\frac{\partial^2 f(u_2)}{\partial u_2{}^2} \rangle\ 0$$

[Eqs 16]

We find that for u_1 =b this condition is held. What has been done is to prove the optimal LA both geometrically and analytically. In IMRT it is practical to carry out a beamlet-discretization to set the angle limits more accurately. This method yields a refinement in the LA upper boundaries. The straight lines that define the lower boundaries of the wedge volume are two. One lateral with the same gradient of the inferior plane of the wedge and other perpendicular to this largest wall zone which is the border of the broad part of the wedge. The equations of the straight lines are not complicated to be determined through analytic geometry. In that way, the distances among the collimator output (P), beamlet by beam let to discretized points of these lines can be also calculated. We refer this formulation to subsequent publications, and set this initial point for dose delivery precision in software/planning IMRT. Now we proceed to apply the same concept on the previous [11] method of beam divergence angle decomposition.

DECOMPOSITION-APPROXIMATIONS.SOME MATHEMATICAL COMPARISONS

In Fig 4 we show the decomposition of main divergence angle as in [1], to carry out a further approximations, as we made in [Eq 1]. Then we get

for θ1

$$\frac{(P + 2c)}{a} = \frac{P}{r_1};$$

that is

$$r_1 = \frac{(a \cdot P)}{(P + 2c)};$$

or

$$tg\theta_1 = \frac{r_1}{P} = \frac{a}{(P + 2c)};$$

with

$$\theta_1 = arctg\left[\frac{a}{(P + 2c)}\right];$$

now with θ_2

$$\frac{(P + c)}{a} = \frac{P}{r_2};$$

ISSN: 2277-3754
ISO 9001:2008 Certified
International Journal of Engineering and Innovative Technology (IJEIT)
Volume 3, Issue 7, January 2014

$$tg\theta_2 = \left[\frac{(P+c)}{a}\right]^{(-1)} = \left[\frac{P}{r_2}\right]^{(-1)};$$

therefore

$$\theta_2 = arctg\left[\frac{a}{(P+c)}\right];$$

[Eqs 17]

Therefore, to make sure the components of the decomposed beam have a correct output point the following conditions should hold

$$\theta_1 \le arctg\left[\frac{a}{(P+2c)}\right];$$

and

$$\theta_2 \le arctg\left[\frac{a}{(P+c)}\right];$$

[Eqs 18]

Then, we have determined the mathematical and geometrical conditions when using beam-decomposition angles. Any beam whose decomposed angles accomplish this is confined into the right path when emerging from the inferior part of the wedge. We step forward to explain another approximation calculated at the inferior plane of the wedge, Fig 8, taking the coordinates of the emerging beam/beamlet. We get r as beamlet position of the emergent beam in this quadrant, such as,

$$r^2 = r_1{}^2 + r_2{}^2 \le b^2;$$

then,

$$u_1 = \frac{(P \cdot r_1)}{(P+2c)}; \qquad u_2 = \frac{(P \cdot r_2)}{(P+2c)};$$

and we decompose the beam/beamlet angle,

$$\tan\theta_2 = \frac{u_2}{P}; \qquad \tan\theta_1 = \frac{u_1}{P};$$

$$\tan\theta = \frac{r}{(P+2c)};$$

Hence we get,

$$\frac{(P+2c)^2}{P^2} \cdot \left[P^2 \tan\theta_1{}^2 + P^2 \tan\theta_2{}^2\right] \le b^2;$$

or

$$\tan^2\theta = \tan^2\theta_1 + \tan^2\theta_2 \le \frac{b^2}{(P+2c)^2};$$

[Eqs 18.1]

And these formulas are also useful for complementary determinations both for theoretical dose delvery and planning system. We refer the 3D formula defined in [11, an example in Table 1] for wedge filters path using decomposition is

$$D^2 = \left[u_1 - \frac{\tan\theta_1 a(-\sin\alpha)}{\tan\theta_1 \sin\alpha - \cos\alpha}\right]^2 + \left[u_2 - \frac{\tan\theta_2 a(-\sin\alpha)}{\tan\theta_1 \sin\alpha - \cos\alpha}\right]^2 + \left[\frac{a(-\sin\alpha)}{\tan\theta_1 \sin\alpha - \cos\alpha}\right]^2 \qquad \text{[Eq 19]}$$

and the approximation for small angles [11]

$$D^2 \cong \left[u_1 - \frac{\theta_1 a(-\sin\alpha)}{\theta_1 \sin\alpha - \cos\alpha}\right]^2 + \left[u_2 - \frac{\theta_2 a(-\sin\alpha)}{\theta_1 \sin\alpha - \cos\alpha}\right]^2 + \left[\frac{a(-\sin\alpha)}{\theta_1 \sin\alpha - \cos\alpha}\right]^2$$

Then, we can use these previous angle limits to optimize this equation making sure that the path is exact and at the same time the output of the beam is correctly set. Previously, [35, Fig 6] it was set a 2D approximation whose experimental results are good. Given this AAA model in water, with the photon-fluence approximation
with

$$D(x,y,z) = I(z) \int_{-\infty}^{+\infty}\int_{-\infty}^{+\infty} \Phi(u,v,z) \cdot \sum_{k=1}^{3} \frac{c_k}{\pi\sigma_k^2(z)} \exp[-((x-u)^2 + (y-v)^2)/\sigma_k^2(z)]\, du\, dv$$

[Eqs 20. From Ref 35]

We explain the physical-mathematical significance of the convolution within the integral dose for better learning. If we fix a point (x,y), the exponential becomes maximum (equal to unity) when the u,v coordinates take that same value (straight direction, maximum quantity of photons). And the minimum value of the exponential is when the u,v values

ISSN: 2277-3754
ISO 9001:2008 Certified
International Journal of Engineering and Innovative Technology (IJEIT)
Volume 3, Issue 7, January 2014

have the same sign and highest value (opposite part of teh beam and minimum fluence of photons coming from that zone).

where with a beam of cross-section 2a x 2b and

$$a' = a \cdot \left(1 + \frac{z}{F}\right);$$

[Fig 6]

and

$$b' = b \cdot \left(1 + \frac{z}{F}\right);$$

the fluence approximation for wedge filters from Ulmer and Harder (1996),

$$\Phi_w(u,v,z) = \Phi_u(u,v,z) \cdot \exp[-\mu_w \left(L \pm \frac{cu}{F+z}\right) \frac{\sin\alpha}{\cos(\alpha+\varphi)}]$$

[Eqs 21.From Ref 35]

and the classical fluence equation developed by Ulmer and Harder after integration of erf functions (1996),

$$\Phi_w(u,v,z) = \Phi_u(u,v,z)\ A \exp(-2qu)$$

with

$$A = \exp\left(-\mu_w L \frac{\sin\alpha}{\cos(\alpha+\varphi)}\right) \text{ and}$$

$$2q = \pm \left(\frac{\mu_w c}{F+z}\right) \frac{\sin\alpha}{\cos(\alpha+\varphi)}$$

[Eqs 22. From Ref 35] with the final convolution for the dose in 2D

$$D(x,y,z) = \frac{\Phi_0 I(z) A}{4(1+z/F)^2} \sum_{k=1}^{3} c_K \exp(\sigma_k^2 q^2 - 2qx) \bullet$$
$$\bullet \left(erf\left(\frac{y+b'}{\sigma_k}\right) - erf\left(\frac{y-b'}{\sigma_k}\right)\right)$$
$$\bullet \left(erf\left(\frac{x+a'-\sigma_k^2 q}{\sigma_k}\right) - erf\left(\frac{x-a'-\sigma_k^2 q}{\sigma_k}\right)\right)$$

[Eq 23. From Ref 35]

Given a previously further approximation

$$\mu = \mu' (1 - C_w L \tan\alpha)$$

Where the constants C_w are tabulated [35].

[Eq 24. From Ref 35]

We will develop the variable transformation that was carried out to handle the integration of [Eqs 22]. To get the solution as shown in [Eq 23] we need to build a binomial different from those of [Eqs 20].Then, A does not depend on u or v, therefore it is constant, but 2q is a factor of u, therefore
[Eq 25]

matematical terms to form a binomial are,

$$[x-(u-\sigma^2 q)]^2 = x^2 - u^2 - \sigma^4 q^2 + 2u\sigma^2 q - -2xu + 2xq\sigma^2$$

we have all these terms with the exception of the third and the last one.Then we have to sum $+\sigma^4 q^2$ *and* $-2qx\sigma^2$ *and all is completed, the transformation gives* [Eq 23].

The result of these transformations is the first exponential in [Eq 23. From Ref 35]. This is the reason to explain the variations at erf functions of x in [Eq 23. From Ref 35]. The angle φ in [eq 21 From Ref 35.] is equivalent to theta angle in Figs 1-4. Alpha in [Eq 21. From Ref 35] is also the wedge angle. In [Eq 21. From Ref 35], note that if we treat this problem in 2D, there is always an error depending on coordinate v (through the plane of the image). In [Eq 21. From Ref 35] c is equivalent to P in our 3D formula [Figs 1-3, and 6], and z coordinate origin is taken lower at a distance P-C from the superior plane of the wedge and towards the patient surface. The distance L corresponds to the distance a in Figs 1-6. With these equivalences it is possible to set mathematical links between one model and the other.

III. APPLICATIONS FOR CONFORMAL WEDGES

In previous contributions [9,10,11], the LA was mathematically defined and developed for wedges. We detail here the main formulas and one sketch of LA, together with a picture of the so-called Conformal Wedge [11.1, 11.2]. A Conformal Wedge Filter has a sloping geometry divided into several non-continuous steps. The dose distribution in these types of wedges changes its shape for a more conformal radiation distribution, if the tumor presents irregular geometry/contour, rather non-spherical.The Conformal Radiotherapy Wedge was mathematically/physically designed by F Casesnoves (July 2005,Madrid City). Computational/Numerical Simulations were carried out at Denver, October 2012 (Patent in Pending Process). The wedge filter function is to attenuate the radiation beam in increasing magnitude, usually along the transversal direction to the photon-

ISSN: 2277-3754
ISO 9001:2008 Certified
International Journal of Engineering and Innovative Technology (IJEIT)
Volume 3, Issue 7, January 2014

beam. As a result, the dose delivery magnitude forms a curved distribution in that transversal direction for each radiation-depth value within the photon dose-deposition region. Classical wedges geometry have a straight sloping face corresponding to the hypothenuse of the triangle defined by the lateral sides. As was detailed previously, ggiven a fixed collimator output to wedge surface distance, LA is defined as the maximum angle of divergence that can be reached by the whole radiation beam without emerging at any point of lateral walls of the wedge. Photon-Beam divergence angles values vary around 20 degrees. The Beam minimum divergence depends on the collimator design quality, and in general of the precision engineering manufacturing of the LINACs. LA in conformal wedges is useful because of several reasons. Avoids hot spots, sub-optimal dose delivery, planning system software propagation errors, overdose at OARS, and repetition of planning work caused by sub-optimal dose delivery calculations. The LA for a conformal wedge calculation presents some additional difficulties. However, the primary approximation is to take as LA for a Conformal Wedge the value of the deepest step of the wedge. In Fig 7 we show a basic sketch of a conformal wedge.

IV. COMPUTATIONAL SOFTWARE

Several subroutines of Optimization Methods were used to check the accuracy of the mathematical formulation (Freemat, GNU, General Public License,Samit Basu). In particular, for geodesics curves we used polynomial subroutines. The graphics were useful to obtain imaging representations of the algorithms developed, plotting the path length related to divergence angle.

V. RESULTS AND FORMULATION

We have shown a summary of formulas useful, in general, for 15, 30, 45, and 60 standard wedge filters. Collimator output distance to wedge surface is given by variable P. We consider the results as an initial approximation in order to obtain more applicable/evolutioned algorithms for planning precision. Other use of the formulation could be focused on MLC techniques with/without wedges, static or dynamic. Conformal Wedges Formulation will be developed in further contributions [Fig 7]. All in all, formulas were made in a practical sense for cancer RT treatment planning.

VI. DISCUSSION AND CONCLUSIONS

Limit Angle data for Photon–Beam Divergence determination is useful when using wedge filters for conformal dose delivery. LA mathematical formulation is especially practical for high-divergent or poorly-collimated beams, and rather long-distance from collimator output to wedge filters (or any BMD of similar geometrical attenuation in general). If the beam is located properly over the wedge surface, the possibility to create hot spots in dose delivery can be reduced. LA is useful because of several reasons. Avoids hot spots and overdose, sub-optimal dose delivery, planning system software propagation errors, overdose at OARS, and repetition of planning work caused by sub-optimal dose delivery calculations.

The mathematical formulation/approximations presented can be considered a primary acceptable stage for overcoming this kind of technical problems in Radiation Therapy Inverse Treatment Planning, improving dose delivery optimization in superficial tumors (lung, breast, etc) and avoiding hot spots. LA formulation could also be appropriate for computational design of Planning Systems and Inverse/Forward Optimization Software. Finally, we presented a primary approximation in LA for Conformal Wedges (Casesnoves, 2005).

Therefore, the mathematical development was done to set useful boundaries for confining the beam/IMRT-beam lets within the functional part of the wedges [Figs, 1,2,3,4]. In addition, we set boundaries for beam-decomposition angles, and related these limits with the principal divergence angles. What is more, it was explained the mathematical equivalence between the classical AAA/2D wedge formulation and the 3D equations that have been developed [11 and Figs 5,6].In fact, not only one exclusive geometrical method was used, but also different techniques to confine the beam/IMRT-beam lets within the optimal dose delivery zone. The initial approximations for conformal wedge fiters involve promising approaches to be carried out.

The future applications of this mathematical framework show a number of alternatives. Among them, the industrial manufacturing/design of other types of BMD.The engineering precision for wedges/MLCs//LINACS, or BMD combinations. The improvement of the therapy treatment and the reduction of manufacturing economic cost. Besides, these equations constitute to enhance the design of the prospective conformal wedges.

To summarize, we presented for sharp learning in this contribution, a series of geometrical-mathematical formulation with both medical and industrial applications. We have set future perspectives for the new design of radiotherapy BMD/apparatus and other new types of BMD, such as the conformal wedge, to be developed in future.

REFERENCES

[1].-Ahnesjö A.,Saxner M., A. Trepp. A pencil beam model for photon dose calculations. Med. Phys. 19, 263-273, 1992.

[2].-Brahme, A. Development of Radiation Therapy Optimization.Acta Oncologic Vol 39, No 5, 2000.

[3].-Bortfeld, T et al. Multicriteria optimization in IMRT planning. Laboratory Report, Fraunhofer-Institut für techno- und Wirtschaftsmathematik ITWM, 2005.

[4].-Barry, D. 'Dynamic Wedge Dosimetry on a Dual Energy Linear Accelerator'. MSc Thesis. McGill University, Dept Medical Physics. 1996.

[5].-Censor Y, and S A Zenios. Parallel Optimization: Theory, Algorithms and Applications. UOP, 1997.

ISSN: 2277-3754
ISO 9001:2008 Certified
International Journal of Engineering and Innovative Technology (IJEIT)
Volume 3, Issue 7, January 2014

[6].-Casesnoves, F. 'Determination of absorbed doses in common radio diagnostic explorations'.5th National Meeting of Medical Physics. Madrid, Spain. September 1985.

[7].-Casesnoves, F. Bachelor Thesis, 'A triple Gaussian pencil beam model for Radiation Therapy Treatment Planning'. Kuopio University. Radiotherapy Department of Kuopio University Hospital and Radiotherapy Physics Group. Finland. 2001.

[8].-Casesnoves, F. Master Thesis, 'A theoretical description of an optimization algorithm for static wedges in radiotherapy'. Radiotherapy Department of Kuopio University Hospital and Radiotherapy Physics Group. Finland. 2001.

[9].-Casesnoves, F. 'Large-Scale Matlab Optimization Toolbox (MOT) Computing Methods in Radiotherapy Inverse Treatment Planning'. High Performance Computing Meeting. Nottingham University. January 2007.

[10].-Casesnoves, F. 'A Computational Radiotherapy Optimization Method for Inverse Planning with Static Wedges'. High Performance Computing Conference. Nottingham University. January 2008.

[11].-Casesnoves, F.'Exact/Approximated Geometrical Determinations of IMRT Photon Pencil-Beam Path through Alloy Static Wedges in Radiotherapy Using the Anisothropic Analytic Algorithm (AAA)'. ASME Denver Conference of Mechanical Engineering. Denver 2011, USA. IMECE2011-65435.

[11.1] Casesnoves, F 'Geometrical Determinations of Limit Angle (LA) related to Maximum Pencil-Beam Divergence Angle in Radiotherapy Wedges' Casesnoves, F.Peer-reviewed ASME Conference Paper. ASME 2012 International Mechanical Engineering Congress.Houston.Nov 2012.USA.IMECE2012-86638.

[11.2] 'A Conformal Radiotherapy Wedge Filter Design. Computational and Mathematical Model/Simulation' Casesnoves, F. Peer-Reviewed Poster IEEE (Institute for Electrical and Electronics Engineers), Northeast Bioengineering Conference. Syracuse New York, USA. Presented in the Peer-Reviewed Poster Session on 6th April 2013. Sessions 1 and 3 with Poster Number 35. Page 15 of Conference Booklet. April 6th 2013

[12].-Censor, Y. Mathematical Optimization for the Inverse problem of Intensity-Modulated Radiation Therapy. Laboratory Report, Department of Mathematics, University of Haifa, Israel, 2005.

[13].-Capizzello and Others. Adjuvant Chemo-Radiotherapy in Patients with Gastric Cancer. Indian Journal of Cancer, Vol 43, Number 4. 2006.

[14].-Do, SY, and Others. Comorbidity-Adjusted Survival in Early Stage Lung Cancer Patients Treated with Hypo fractioned Proton Therapy. Journal of Oncology, Vol 2010.

[15].-Ehrgott, M, Burjony, M. Radiation Therapy Planning by Multicriteria Optimization. Department of Engineering Science. University of Auckland. New Zealand.

[16].-Ezzel, G A. Genetic and geometric optimization of three dimensional radiation therapy treatment planning. Med.Phys.23, 293-305.1996.

[17].-Effective Health Care, Number 13. Comparative Effectiveness of Therapies for Clinically Localized Prostate cancer. 2008.

[18].-Haas, O.C.L.Radiotherapy treatment planning, new systems approaches. Springer Engineering.1998.

[19].-Hansen, P. Rank-deficient and discrete ill-posed problems: numerical aspects of linear inversion. SIAM monographs on mathematical modeling and computation, 1998.

[20].-Hashemiparast, SM, Fallahgoul, H. Modified Gauss quadrature for ill-posed integral transform. International Journal of Mathematics and Computation. Vol 13, No. D11. 2011.

[21].-Harari, P, and others. 'Improving dose homogeneity in routine head and neck radiotherapy with custom-3D compensation'. Radiotherapy and Oncology. 49. 1998.

[22].-Johansson, K-A et al. Radiation Therapy Dose Delivery.Acta Oncologic Vol 42, No 2, 2003.

[23].-Jiandong, R and Yumping, Z. 'Selecting beam weight and wedge filter on the basis of dose gradient analysis'. Med. Phys. 27 (8). 2000.

[24].-Kufer,K.H. et al. A multicriteria optimization approach for inverse radiotherapy planning. University of Kaiserslautern, Germany.

[25].-Kirsch, A. An introduction to the Mathematical Theory of Inverse Problems. Spinger Applied Mathematical Sciences, 1996.

[26].-Luenberger D G. Linear and Nonlinear Programming 2nd edition. Addison-Wesley, 1989.

[27].-Moczko, JA, Roszak, A. application of Mathematical Modeling in Survival Time Prediction for Females with Advanced Cervical cancer treated Radio-chemotherapy. Computational Methods in Science and Technology, 12 (2). 2006.

[28].-Mohan, R. 'Monte Carlo Simulation of radiation Treatment machine Heads'. Research Report. Memorial Sloan-Kettering Cancer Center. New York. USA.

[29].-Numrich, RW. The computational energy spectrum of a program as it executes. Journal of Supercomputing, 52. 2010.

[30].-Ragaz, J, and Others. Locoregional Radiation Therapy in Patients with High-risk Breast Cancer Receiving Adjuvant Chemotherapy: 20-Year Results of the Columbia Randomized Trial. Journal of National Cancer Institute, Vol 97, Number 2.2005.

[31].-Steuer, R. Multiple Criteria Optimisation: Theory, Computation and Application. Wiley, 1986.

[32].-Spirou, S.V. and Chui, C.S. A gradient inverse planning algorithm with dose-volume constraints. Med. Phys. 25, 321323.1998.

[33].-Sharma, SC. Beam Modification Devices in Radiotherapy. Lecture at Radiotherapy Department, PGIMER. 2008.

[34].-Ulmer, W, and Harder, D. A triple Gaussian pencil beam model for photon beam treatment planning. Med. Phys. 5, 2530, 1995.

[35].-Ulmer, W, and Harder, D. Applications of a triple Gaussian pencil beam model for photon beam treatment planning. Med.Phys. 6, 68-74, 1996.

[36].-Ulmer, W. A 3D photon superposition/convolution algorithm and its foundation on results of Monte Carlo calculations. Phys. Med. Biol. 50, 2005.

ISSN: 2277-3754
ISO 9001:2008 Certified
International Journal of Engineering and Innovative Technology (IJEIT)
Volume 3, Issue 7, January 2014

[37].-Ulmer, W et al. Laboratory Report. Phys. Med. Biol. 50, 2005.

[38].-Ulmer, W, and Harder, D. Applications of the triple Gaussian Photon Pencil Beam Model to irregular Fields, dynamical Collimators and circular Fields, 1997.

[39].-Ulmer, W, Schaffner, B. Foundation of an analytical proton beamlet model for inclusion in a general proton dose calculation system. Radiation Physics and Chemistry, 80. 2011.

[40].-Valachis, A, and Others. Partial Breast Irradiation or Whole Breast Radiotherapy for Early Breast Cancer: a Meta-Analysis of randomized controlled Trials. The Breast Journal, Vol 16, Number 3. 2010.

[41].-Vinagre, F, Simoes, P, Rachinhas, P. 'Ommni-Wedge Technique for increased dose homogeneity in head and neck Radiotherapy'. Physica Medica. 2009.

ANNEX A. BASIC GEOMETRIC PICS/SKETCHES

Figures 1 (upper) and 2.- Geodesic calculations method. Upper pic shows the starting point to trace the curve. Pic 2 the final point at the plane quadrant.

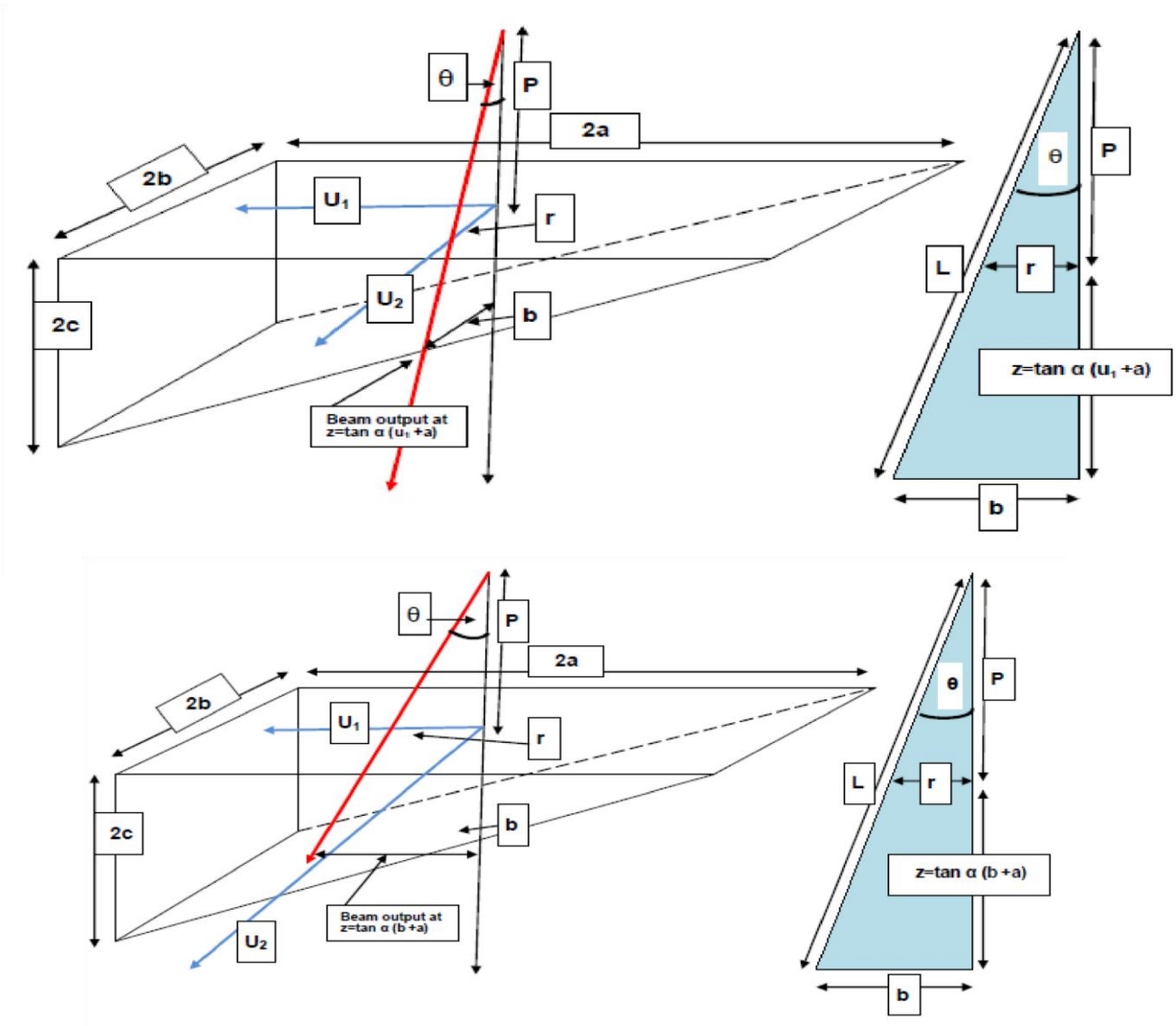

ISSN: 2277-3754
ISO 9001:2008 Certified
International Journal of Engineering and Innovative Technology (IJEIT)
Volume 3, Issue 7, January 2014

Figures 3 (upper) and 4.- Geodesic calculations method, with cylinder intersection. Lower pic shows the Decomposition Approximation.

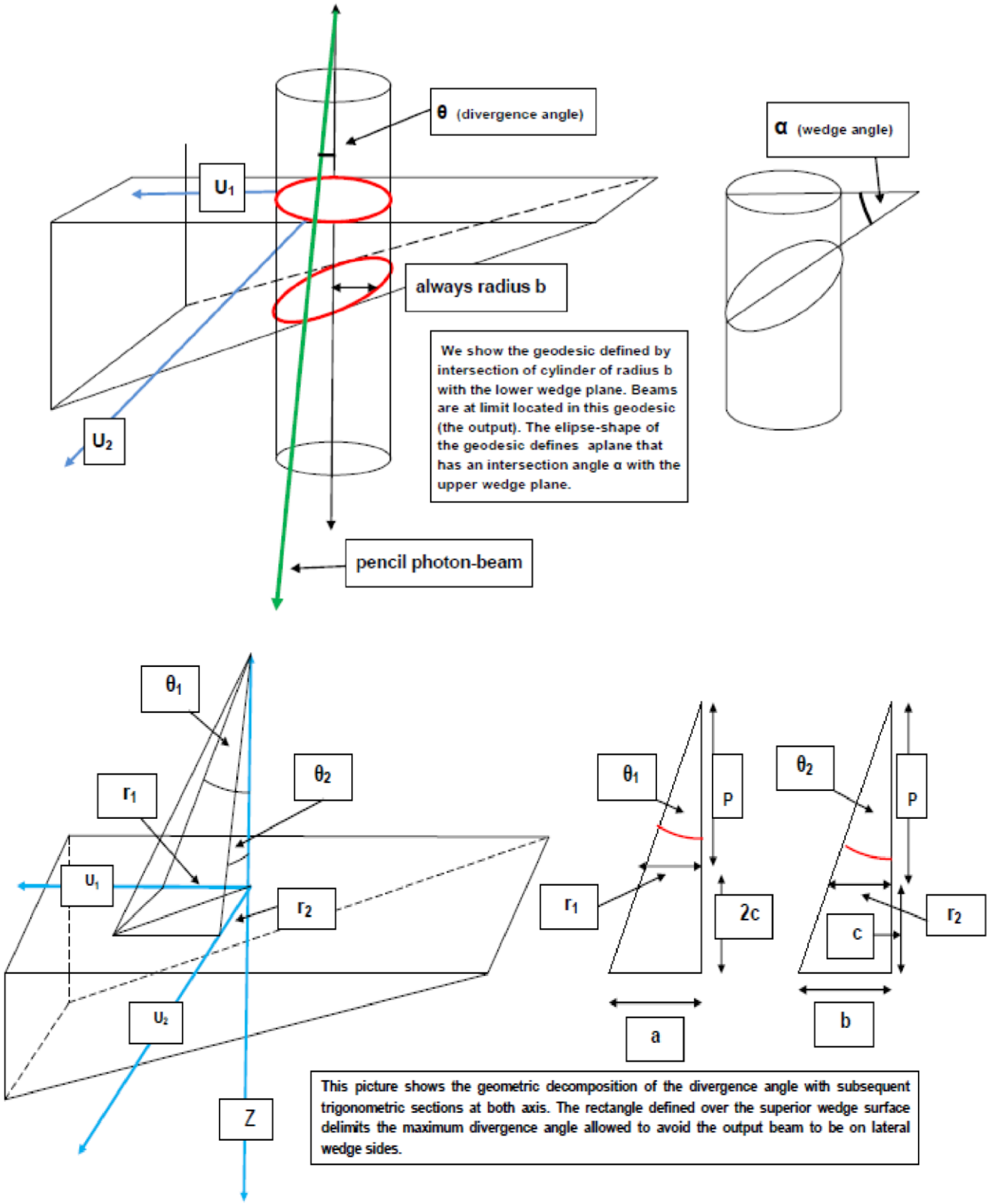

ISSN: 2277-3754
ISO 9001:2008 Certified
International Journal of Engineering and Innovative Technology (IJEIT)
Volume 3, Issue 7, January 2014

Fig 5.-This sketch [11] shows with more detail the beam decomposition that was used in previous contributions to determine the exact/approximated path of the pencil beam through the wedge.

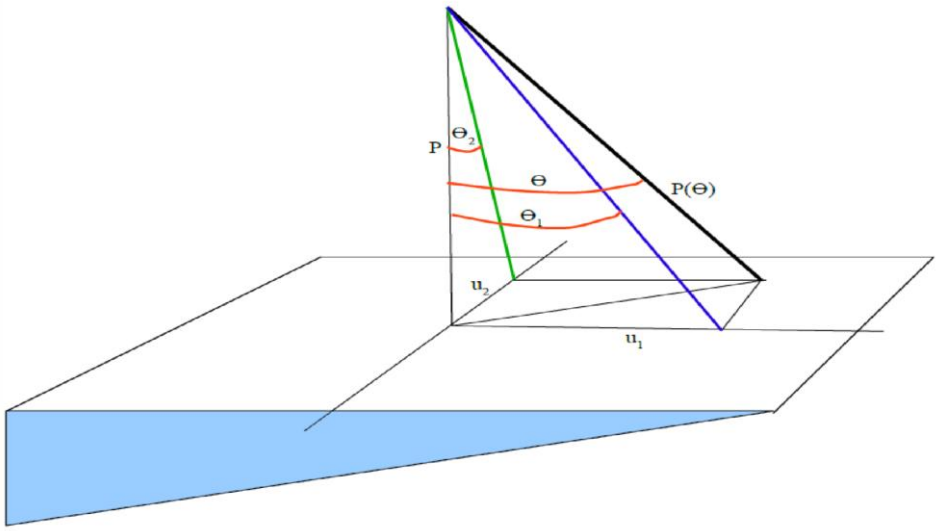

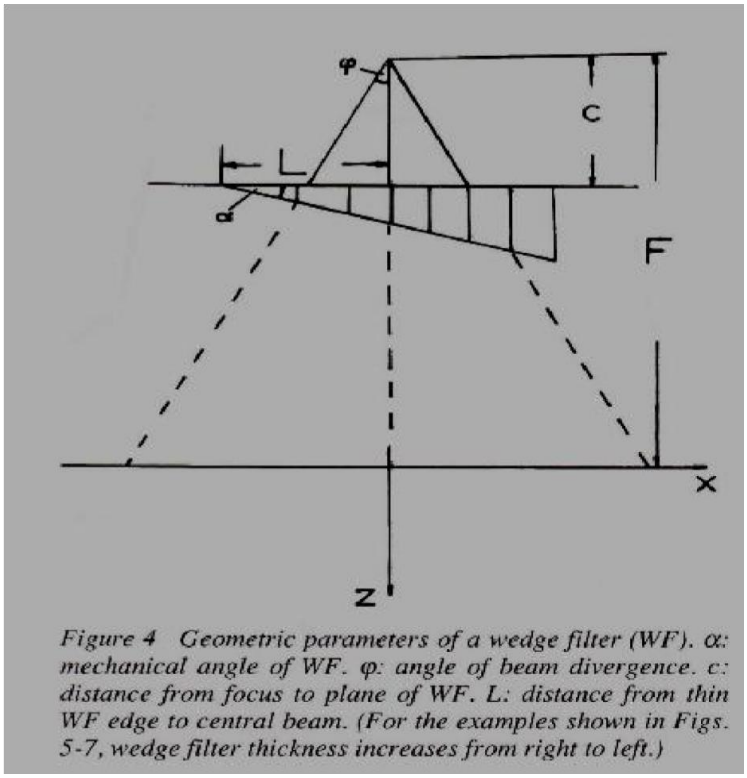

Figure 4 Geometric parameters of a wedge filter (WF). α: mechanical angle of WF. φ: angle of beam divergence. c: distance from focus to plane of WF. L: distance from thin WF edge to central beam. (For the examples shown in Figs. 5-7, wedge filter thickness increases from right to left.)

Fig 6.-2D approximation for wedge filters by Ulmer and Harder [35]. This approximation has acceptable experimental results that corroborate the formula [21]. But note that if we treat this problem in 2D, there is always an error depending on coordinate v (through the plane of the image).

ISSN: 2277-3754
ISO 9001:2008 Certified
International Journal of Engineering and Innovative Technology (IJEIT)
Volume 3, Issue 7, January 2014

Figs 7 and 8.-Basic Sketch of a Conformal Wedge, upper [11.1,11.2]. Geometrical analysis corresponding to Equations 18.1.

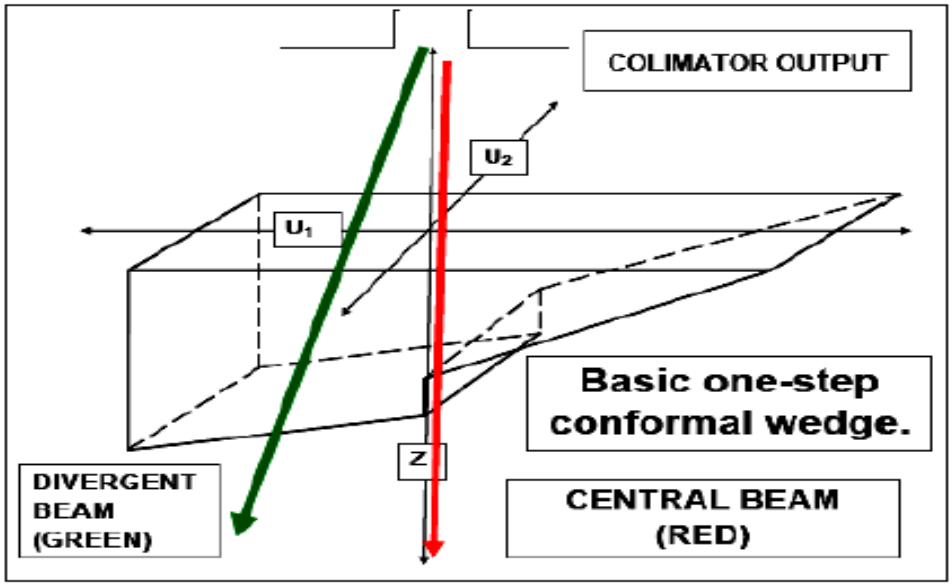

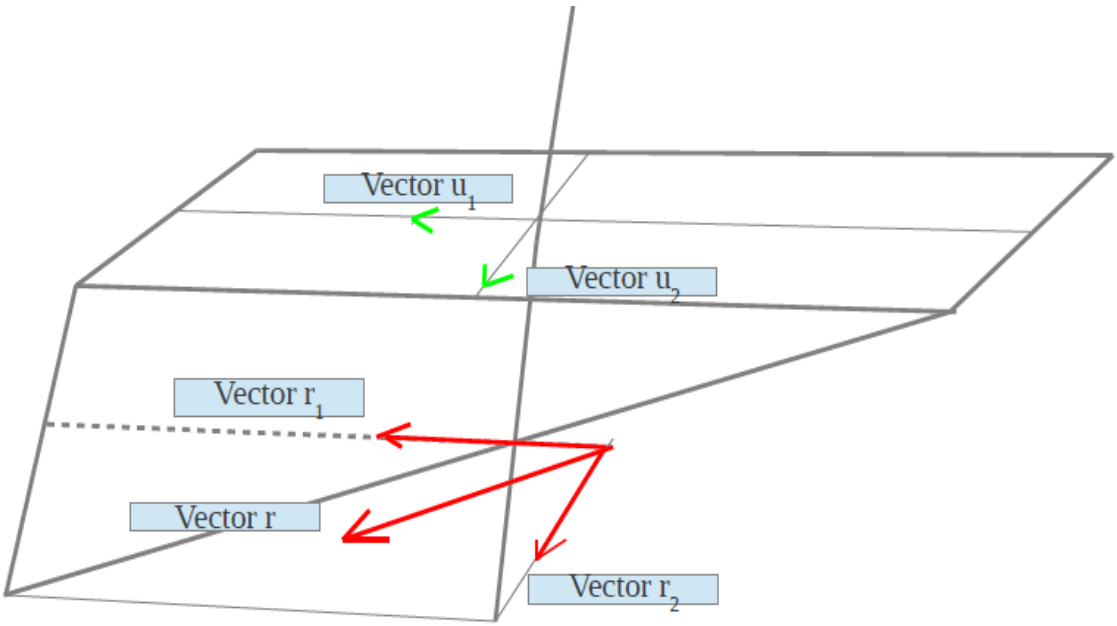

ISSN: 2277-3754
ISO 9001:2008 Certified
International Journal of Engineering and Innovative Technology (IJEIT)
Volume 3, Issue 7, January 2014

SIMULATIONS RESULTS FOR 30° WEDGE (Standard Manufacturing Size)							
ANGLE=30°	P=20cm	d=15 x tan30°= =8.6603cm d=Central Depth	a=15cm	b=10cm	c=17.3205cm	Hypotenuse= = 34.6410cm	Comment: results with simple precision, and Limit angle rather small
SIMULATION	RANDOM P_0 COORDINATES (cm) (1)u_1 (2)u_2	ANGLES (Radians) (1) θ_1 (2) θ_2	(1) L_K EXACT (cm) (2) L_K APPROX (cm)	ABSOLUTE ERROR MAGNITUDE 10^{-x} (cm)	ABSOLUTE ERROR Exact-Approx Magnitude sign	DIFFERENCE (cm x 10^{-2})	COMMENTS In general, when the wedge angle is small we find lower RMS Errors. Simulations ranges to avoid Limit Angle, $u_1 \in [0,10]$ $u_2 \in [0,5]$
1	1.-3.7595 2.-2.6566	1.-0.1858 2.-0.1321	1.-9.9988 2.-9.9914	-3	+	0.7400	All these value shows small differences, probably not exceeding the Limit Angle, At the thick part of the wedge
2	1.-0.1834 2.-4.9790	1.-0.0092 2.-0.2440	1.-9.1418 2.-9.1631	-2	-	-1.3300	
3	1.-9.1342 2.-1.0396	1.-0.4284 2.-0.0519	1.-12.3561 2.-12.2584	-1	+	9.7700	
4	1.- 3.5799 2.- 2.4605	1.-0.1771 2.-0.1224	1.-9.9161 2.-9.9095	-2	+	0.6600	
5	1.-7.6040 2.-3.7984	1.-0.3633 2.-0.1877	1.-11.7283 2.-11.6728	-1	+	5.0500	
6	1.-8.0768 2.-1.6824	1.-0.3838 2.-0.0839	1.-11.8638 2.-11.7826	-1	+	8.1200	
7	1.-0.9900 2.-4.3384	1.-0.0495 2.-0.2134	1.-9.2506 2.-9.2581	-3	-	-0.7500	
8	1.-4.9723 2.-1.3570	1.-0.2437 2.-0.0677	1.-10.4280 2.-10.4095	-2	+	1.8500	
9	1.-3.4781 2.-1.0870	1.-0.1722 2.-0.0543	1.-9.8107 2.-9.8037	-2	+	0.7000	High precision in Approximations, very low Relative Error
10	1.-0.2764 2.-3.4485	1.-0.0138 2.-0.1707	1.-8.9449 2.-8.9481	-3	-	-0.3200	RELATIVE ERROR 0.43%
AVERAGE	N/A	N/A	L_K EXACT (cm) Average: 10.3442	Approx (-2)	+	-	RMS ERROR [0.0441]

Table 1.-Example of table with simulations of distance through standard wedge presented in previous publications [11].